Drop vaporization frequency response: an approximate analytical solution for mixed injection regimes

Réponse en fréquence de l'évaporation des gouttes : une solution analytique approximative pour les régimes d'injection mixtes

Kwassi Anani[1,*], Roger Prud'homme[2] and Mahouton Norbert Hounkonnou[3]

[1] Doctor, Laboratory of Mathematical Modelling and Applications, Department of Mathematics, Faculty of Sciences, University of Lomé, kanani@univ-lome.tg

[2] Emeritus Research Director, Jean Le Rond d'Alembert Institute, UMR 7190 - Sorbonne University / Centre National de la Recherche Scientifique, roger.prud_homme@courriel.upmc.fr

[3] Professor, University of Abomey-Calavi, International Chair in Mathematical Physics and Applications (ICMPA-UNESCO Chair), Republic of Benin, norbert.hounkonnou@cipma.uac.bj

ABSTRACT. The vaporisation frequency response due to pressure oscillations is analysed for a spray of repetitively injected drops into a combustion chamber. In the Heidmann analogy, this vaporizing spray is represented by the so-called 'mean droplet', which is a continuously fed spherical droplet at rest inside the combustion chamber. Only radial thermal convection and conduction effects are considered inside the vaporizing mean droplet since the feeding is realized symmetrically with the same liquid fuel, using a point source placed at the centre. This feeding process, at some liquid-liquid heat transfer coefficient, is now considered as a proper boundary condition of the generalized feeding regime, which controls the whole fuel injection process into the chamber. Effects due to the variation of the heat transfer coefficient are analysed for the evaporating mass response factor, calculated on the basis of the Rayleigh criterion. A chaotic response is especially noticed in the process when the heat transfer coefficient is fixed at unity.

RÉSUMÉ. La réponse en fréquence de l'évaporation de masse aux oscillations de pression est analysée pour un jet de gouttes répétitivement injectées dans une chambre de combustion. Dans l'analogie de Heidmann, ce jet de gouttes en évaporation est représenté par la 'goutte moyenne' qui est une goutte sphérique continuellement alimentée placée dans la chambre de combustion. L'alimentation est réalisée avec un coefficient de transfert thermique liquide-liquide en employant un point source placé au centre de la goutte, de telle manière que seuls les effets radiaux de convection et de conduction thermiques soient pris en compte à l'intérieur de la gouttelette pendant le processus. Ce procédé d'alimentation est maintenant regardé comme représentant un régime d'alimentation généralisé du processus réel d'injection de combustible liquide dans une chambre de combustion. Utilisant une analyse linéaire basée sur le critère de Rayleigh, le facteur de réponse en masse d'évaporation est évalué. Les effets dus à la variation du coefficient de transfert thermique sont analysés. En particulier, une réponse chaotique est notée dans le système quand le coefficient de transfert thermique est fixé à un.

KEYWORDS. heat transfer coefficient, truncated expansion, double confluent Heun equation, transfer function.

MOTS-CLÉS. coefficient de transfert thermique, développements limités, équation doublement confluente de Heun, fonction de transfert.

1. Introduction

Combustion instabilities related to pressure oscillations are due to the coupling between acoustic waves and other combustion phenomena as evaporation, heating... In confined devices, the coupling between acoustic field and heat or mass release at certain frequency levels may lead to engine failure or other catastrophic consequences [1]. On the contrary, new blends of fuels can be

---

*Corresponding author. Email: kanani@univ-lome.tg

engineered to undergo preferential instabilities leading to homogeneous combustion with higher efficiency [2]. The present paper aims at contributing to the linear analysis of subcritical combustion instabilities in diffusion flame models, by analytical approaches based on the mean spherical droplet configuration as in [3]. In the following section, a brief description is made of the unperturbed state corresponding to the vaporization of the continuously fed spherical droplet in a stable environment. In Section 3, the linear analysis for harmonic perturbations in pressure is performed and a double confluent Heun equation (see [4]) is derived from the energy equation of the liquid phase. An approximate analytical expression of the temperature profile inside the mean droplet is then obtained for the generalized or mixed injection regime and the mass response factor is defined. Results are discussed in Section 4 and briefly recalled in the conclusion.

2. Stabilized state description

2.1. *General assumptions*

Individual spherical fuel droplets are repetitively injected into a subcritical combustion chamber. The distance between the droplets is supposed large enough, so that no interaction occurs between the droplets or between the droplets and the wall. Assuming velocity-stabilized hypotheses as in [5], the liquid fuel vaporizing spray is represented in an idealized physical configuration by a mean spherical droplet at rest in the combustion chamber. The mean droplet, placed at a specified location in the combustion chamber (pressure anti-node and velocity node), is supposed to summarize the frequency response of individual drops in the spray. The vaporizing mean droplet has a constant average radius $\bar{r}_S$ since its instantaneous evaporating mass $\dot{M}$ is continuously restored with an average mass flow rate $\overline{\dot{M}}$ of the same fluid by using a point source placed at the centre. The choice of the Arithmetic Mean Diameter configuration is motivated by the analytical approach of the problem since it leads for the mean droplet to conservation equations with fixed boundary conditions. From now on, all barred quantities indicate mean values corresponding to the stabilized state whereas all primed quantities will denote perturbed quantities i.e. $x' = (x - \bar{x}) / \bar{x}$.

The local feeding rate $\overline{\dot{M}}$ is distributed throughout the droplet (see Figure 1(a)) in such a way that, except for the radial thermal convection effect from the droplet centre to its evaporation surface, other convective transport or liquid recirculation phenomenon within the droplet are negligible. The spherical symmetry of the mean droplet is maintained at every moment during the process, and the thermal dilatation of the liquid is negligible so that the density ρ_L, the specific heat c_L and the thermal conductivity k_L of the droplet will be treated as constant. At the mean droplet centre, a generalized or mixed boundary condition is considered, that is the liquid fuel is injected with a positive heat transfer coefficient h. The two extreme cases of this injection process are the adiabatic feeding regime ($h = 0$) where zero temperature gradient is assumed at the droplet centre, and the isothermal feeding regime ($h = \infty$) where the droplet centre is kept at a constant temperature $\overline{T}_S$. The latter is the mean value of the spatially uniform but time-varying temperature T_S of saturated vapour at the stabilized droplet surface.
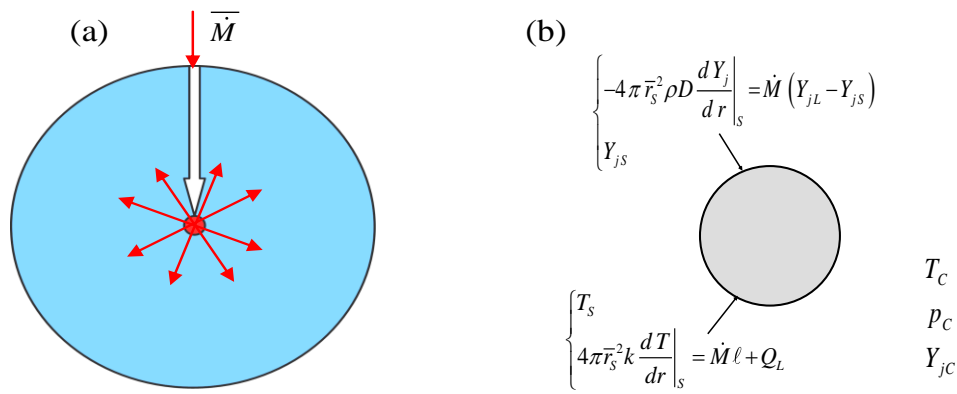
Figure 1. *(a) The mean vaporizing droplet, continuously fed by a point source placed at its centre. (b) Boundary conditions for the supplied droplet.*

In the immediate vicinity of the droplet surface, the gas phase is made up of stoichiometric reaction products evolving in a quasi-steady state. Equilibrium conditions at the droplet/gas interface are assumed for the stabilized state and there is no gas diffusion into the droplet. Far from the mean evaporating droplet, the ambient environment inside the chamber is at constant subcritical temperature T_C and pressure p_C. The boundary conditions at the supplied droplet surface are shown in Figure 1(b). Subscripts L and l refer to liquid phase, whereas subscripts S and C respectively indicate the droplet surface and the conditions for the combustion chamber far from the droplet. The heat flux transferred to the liquid is designated by Q_L and the binary diffusion coefficient of fuel vapour in air is denoted by D. The density and the thermal conductivity of the gas mixture around the droplet surface are respectively designated by ρ and k. The mass fraction of species j being denoted by Y_j, the gaseous mixture near the surface is composed of fuel species $j = F$ and of combustion products diluted species $j = A$ proceeding from the flame front at infinity. For reason of simplicity, we have considered a mono-component droplet with only fuel species, that is $Y_{FL} = 1$ and $Y_{AL} = 0$.

2.2. *Characteristic times*

The residence time of the continuously fed droplet can be equated to the mean lifetime of an individual vaporizing droplet in the spray. This time replaces the notion of the free droplet lifetime in the present situation of constant volume and is identified to the ratio $\bar{\tau}_v = \overline{M} / \overline{\dot{M}}$, where $\overline{M}$ represents the mean value of the actual mass M of the supplied droplet and $\overline{\dot{M}}$ is the stationary feeding rate. The transfer time by thermal diffusion process is defined as $\bar{\tau}_T = \bar{r}_S^2 / \kappa_L$, where $\kappa_L = k_L / (\rho_L c_L)$ is the thermal diffusivity of the liquid and $\bar{r}_S$ the constant average radius. It is then convenient to use the timescale ratio $\theta = 9\bar{\tau}_v / \bar{\tau}_T = \bar{\tau}_v / \tilde{\tau}_T$, which will be called from now on, the thermal exchange ratio or more briefly the exchange ratio, as it is of the same order of magnitude as $1 / Pe_L$, Pe_L being the Péclet number of the liquid phase. The coefficient 9 is kept for comparison purposes with results obtained in [3]. During the vaporization, intrinsic or external pressure-related oscillations can cause departure from stabilized-state conditions. The frequency of such ambient pressure oscillations is a major characteristic time of the process. In the case of small harmonic perturbations in pressure, a linear analysis can be performed. The frequency of the harmonic oscillations in ambient pressure will be denoted by ω. In order to provide a parameter depending on the residence time $\bar{\tau}_v$, which may be used to characterize the frequency response for classical fuels, a reduced frequency u defined as $u = 3\omega\bar{\tau}_v$ will be considered.

2.3. *Unperturbed state equations*

The mass balance of the mean droplet is:

$$\frac{dM}{dt} = \overline{\dot{M}} - \dot{M} \tag{1}$$

with $\overline{\dot{M}}$ denoting the stationary flow of injection and $\dot{M}$ the instantaneous flow of evaporation. In a stabilized state, one has: $\dot{M} \equiv \overline{\dot{M}}$, $dM / dt = 0$ and $M = \overline{M}$.

The amount of heat Q_L penetrating into the droplet is expressed as:

$$4\pi \overline{r}_S^2 \, k_L \left. \frac{\partial T_l}{\partial r} \right|_{\overline{r}_S, t} = Q_L = Q - \dot{M}\ell \tag{2}$$

where $T_l \equiv T_l(r,t)$ is the temperature value at radial coordinate r and at time t inside the mean droplet. The external gas heat flux is denoted by Q and ℓ designates the latent heat of vaporization per unit mass of the liquid. Equation (2) assures the coupling of the gas and the liquid phase solutions at the mean droplet surface. The formulation of the energy conservation equation includes both radial thermal convection and conduction data. In these conditions, the internal temperature T_l satisfies the following equation:

$$\rho_L \, c_L \frac{\partial T_l}{\partial t} + \rho_L \, c_L v_r \frac{\partial T_l}{\partial r} - \frac{k_L}{r} \frac{\partial^2 (r \, T_l)}{\partial r^2} = 0 \tag{3}$$

where v_r is the central injection velocity expressed as $v_r = \overline{\dot{M}} / 4\pi \rho_L r^2$ with $0 < r < \overline{r}_S$.

This equation is solved, subject to the mixed boundary condition at the droplet centre and to the Dirichlet boundary condition at the surface:

$$\begin{cases} \left. \dfrac{\partial T_l}{\partial r} \right|_{r=0,t} = \dfrac{h}{\overline{r}_S} \left(T_l(0,t) - \overline{T}_S \right) \\ T_l(\overline{r}_S, t) = T_S(t) \end{cases} \tag{4}$$

The parameter $h > 0$ indicates the heat transfer coefficient. We recall for the adiabatic centre injection that, $h = 0$ and the mixed boundary condition is reduced to $\partial T_l(0,t)/\partial r = 0$, whereas for the isothermal centre injection, $h = \infty$ and the same condition becomes $T_l(0,t) = \overline{T}_S$.

Assuming quasi-steady hypotheses, the droplet surface is in local evaporation equilibrium and the instantaneous mass vaporization rate can be calculated as:

$$\dot{M} = 2\pi \, \rho \, D \, r_S \, Sh^* \ln(1 + B_M) = 4\pi \frac{k}{c_p} r_S \, Nu^* \ln(1 + B_T) \tag{5}$$

where $B_M = (Y_{FS} - Y_{FC})/(1 - Y_{FS})$ and $B_T = c_p(T_C - T_S)/(\ell + Q_L / \dot{M})$ are the well-known Spalding mass and heat transfer numbers, and c_p the specific heat capacity of fuel vapour at constant pressure. As mentioned above, parameters ρ, k, and D are the density, the thermal conductivity and the binary diffusion coefficient of the mixture of vapour and ambient gas. The Sherwood and Nusselt numbers Sh^* and Nu^* were provided by Abramzon and Sirignano in their extended film model [6]. At the droplet surface, the saturated vapour pressure can be expressed as $p_{sat}(T_S) = \exp(a - b/(T_S - c))$, where

a, b and c are some coefficients related to the fuel thermophysical properties. The pressure p_{sat} and the mole fraction X_{FS} of fuel species are connected by the relation $p\,X_{FS} = p_{sat}(T_S)$, where $p = p_C$ denotes the ambient pressure. If the molecular weight of species $j\,(= A$ or $F)$ is denoted by M_j, then the mass fraction Y_{FS} of the vapour at the droplet surface can be written as a function of the mole fraction X_{FS} as:

$$Y_{FS} = \frac{\mathrm{M}_F}{\mathrm{M}_F X_{FS} + \mathrm{M}_A X_{AS}} X_{FS} \tag{6}$$

Since concentrations and temperature values are evolving in the gas phase, the averaged properties can be evaluated at some reference concentration $\overline{Y}_j = Y_{jS} + A_r\left(Y_{jC} - Y_{jS}\right)$ and temperature $\overline{T} = T_S + A_r\left(T_C - T_S\right)$ with $A_r = 1/3$. Both Sh^* and Nu^* are assumed equal to two and the Lewis number $Le = k/\rho D c_p$ equal to one.

3. Linear analysis for small perturbations

3.1. *Linear analysis of the liquid-phase equations*

Splitting up the flow variables into steady and unsteady parts can be realized by writing $\Delta f = f - \overline{f}$, where f is a flow parameter, $\overline{f}$ is its mean value, Δf is the absolute perturbation, and $f' = \Delta f / \overline{f}$ is the corresponding relative perturbation. The heat flow at the surface, Equation (2), is then given by:

$$4\pi\,\overline{r}_S^2\,k_L\overline{T}_S\,\frac{\partial T_l'}{\partial r}\bigg|_{\overline{r}_S,t} = Q_L = Q_L - \overline{Q}_L = \Delta Q_L \tag{7}$$

as $\overline{Q}_L = 0$. For the perturbed temperature $T_l'(r,t) = [T_l(r,t) - \overline{T}_l(r,t)]/\overline{T}_l(r,t)$, the energy conservation equation, Equation (3), can be rewritten as:

$$\frac{\partial(r T_l')}{\partial t} + \kappa_L\left(\frac{3\overline{r}_S}{\theta r}\frac{\partial T_l'}{\partial r} - \frac{\partial^2(r T_l')}{\partial r^2}\right) = 0 \tag{8}$$

where $\theta = \overline{\tau}_v / \tilde{\tau}_T$ is the thermal exchange ratio (see section 2). The perturbed boundary conditions in the mixed feeding regime are deduced from Equation (4) as follows:

$$\begin{cases} \dfrac{\partial T_l'}{\partial r}\bigg|_{r=0,t} = \dfrac{h}{r_S}T_l'(0,t) \\[2mm] T_l'(\overline{r}_S,t) = T_S'(t) \end{cases} \tag{9}$$

Introducing now small harmonic perturbations of frequency ω in the form of $f' = \hat{f}(r)\exp(\mathrm{i}\omega t)$, the ambient pressure p_C becomes $p' = \hat{p}_C\exp(\mathrm{i}\omega t)$, while the temperature is expressed as $T_l' = \hat{T}_l(r)\exp(\mathrm{i}\omega t)$, and the heat transferred into the droplet as $\Delta Q_L = \Delta\hat{Q}_L(r)\exp(\mathrm{i}\omega t)$. Equation (8) is then transformed into:

$$\mathrm{i} r^2\omega\hat{T}_l + \frac{3\kappa_L\overline{r}_S}{\theta}\frac{\mathrm{d}\hat{T}_l}{\mathrm{d}r} - \kappa_L r\frac{\mathrm{d}^2(r\hat{T}_l)}{\mathrm{d}r^2} = 0 \tag{10}$$

or equivalently into:

$$i\omega \overline{\tau}_T \xi \hat{T}_l + \frac{1}{3\theta\xi} \frac{d\hat{T}_l}{d\xi} - \frac{d^2(\xi\hat{T}_l)}{d\xi^2} = 0 \tag{11}$$

where $\hat{T}_l$ is taken as a function of the reduced radius variable $\xi = r/\overline{r}_S$ ($0 < \xi < 1$). The boundary conditions in the generalized feeding regime, Equation (9), can then be written in connection with ξ as:

$$\begin{cases} \left. \dfrac{d\hat{T}_l}{d\xi} \right|_{\xi=0} = \dfrac{h}{\overline{r}_S} \hat{T}_0 \\ \hat{T}_l(1) = \hat{T}_S \end{cases} \tag{12}$$

where $\hat{T}_0$ depends on the initial temperature of the injected liquid fuel.

We now consider the complex number $\overline{s}_0 = (1-i)(\omega/2\kappa_L)^{1/2}$, conjugate of $s_0 = (1+i)(\omega/2\kappa_L)^{1/2}$, s_0 and $-s_0$ being the roots of the characteristic equation $i\omega - \kappa_L s^2 = 0$ obtained from Equation (10), when neglecting the convective term $(3\kappa_L \overline{r}_S/\theta)d\hat{T}_l/dr$. For any given value of the heat transfer coefficient $h > 0$, a solution of Equation (11) subject to conditions Equation (12) can be sought in the form of $\xi\hat{T}_l(\xi) = J(\xi)\{1 - \cos[\overline{s}_0 \overline{r}_S \xi \exp(i \arctan h)]\}$, with $\exp(i \arctan h) = (ih+1)/(h^2+1)^{1/2}$, and J referring to a function to be determined. From the second-order truncated expansions of sine and cosine functions that are $\sin(S_0\xi) \approx S_0\xi$ and $\cos(S_0\xi) \approx 1 - (S_0\xi)^2/2$ with $S_0 = \overline{s}_0 \overline{r}_S \exp(i \arctan h)$, it is deduced that the function ξJ approximately verifies the following double confluent Heun equation:

$$\xi^2 \frac{d^2(\xi J)}{d\xi^2} + \left(2\xi - \frac{3}{\theta}\right) \frac{d(\xi J)}{d\xi} - 2\overline{s}_0^2 \overline{r}_S^2 \frac{h(i-h)}{h^2+1} \xi^2(\xi J) = 0 \tag{13}$$

By using Maple notation, a solution of Equation (13) can be expressed as: $J(\xi) = C_0 \exp(-3(\theta\xi)^{-1}) \text{HeunD}(x_1, x_2, x_3, x_4, x)/\xi^{\frac{5}{2}}$, where C_0 is an arbitrary constant and $\text{HeunD}(x_1, x_2, x_3, x_4, x)$ is the double confluent Heun function with its corresponding four parameters: $x_1 = 0$, $x_2 = -[\theta^2(h^2+1) - 9 - 9h^2 - 24uh(ih+1)\theta]/4\theta^2(h^2+1)$, $x_3 = -[9 + (9 - 24iu\theta)h^2 - 24hu\theta]/2\theta^2(h^2+1)$ and $x_4 = -[-\theta^2(h^2+1) - 9 - 9h^2 - 24uh(ih+1)\theta]/4\theta^2(h^2+1)$ and the variable $x = (\xi^2 - 1)/(\xi^2 + 1)$. We recall that the quantity $u = 3\omega\overline{\tau}_v$ is the ambient pressure frequency defined in the precedent section. Finally, the condition $\hat{T}_l(1) = \hat{T}_S$ at the mean droplet surface leads for this feeding regime to an approximate analytical solution expressed as:

$$\hat{T}_l(\xi) = \exp\left(\frac{3}{2\theta}\left(1 - \frac{1}{\xi}\right)\right) \frac{\hat{T}_S\{1 - \cos[\exp(i \arctan h)\overline{s}_0 \overline{r}_S \xi]\} \text{HeunD}\left(x_1, x_2, x_3, x_4, \dfrac{\xi^2 - 1}{\xi^2 + 1}\right)}{\{1 - \cos[\exp(i \arctan h)\overline{s}_0 \overline{r}_S]\}\xi^{\frac{5}{2}}} \tag{14}$$

The above approximate analytical solution presents an essential discontinuity at $\xi = 0$, since, once $h > 0$, the temperature gradient is not null at the droplet centre. Now, the calculation of the mass response factor only includes regularity conditions at the droplet surface $\xi = 1$ and these conditions are well verified by this approximate solution. Thus, the flow condition at the droplet surface

(Equation (7)) can be rewritten as $4\pi \bar{r}_S k_L \bar{T}_S \dfrac{\mathrm{d}\hat{T}_l}{\mathrm{d}\xi}\bigg|_{\xi=1} = \Delta\hat{Q}_L$ and then be applied to the solution Equation (14). That leads to:

$$\Delta\hat{Q}_L = -4\pi \bar{r}_S k_L \bar{T} s \hat{T}_S E(u,\theta,h) \tag{15}$$

where E is expressed in function of u, θ and h as:

$$E(u,\theta,h) = \bar{s}_0 \bar{r}_S \exp(\mathrm{i}\arctan h)\frac{\sin[\exp(\mathrm{i}\arctan h)\bar{s}_0 \bar{r}_S]}{\cos[\exp(\mathrm{i}\arctan h)\bar{s}_0 \bar{r}_S]-1} - \frac{3}{2\theta} + \frac{5}{2} \tag{16}$$

with $\bar{s}_0 \bar{r}_S = (1-\mathrm{i})(3u/2\theta)^{1/2}$, $u = 3\omega\bar{\tau}_v$ and $\theta = \bar{\tau}_v / \tilde{\tau}_T$.

3.2. *Gas-phase linearized equations*

The linearized equations for the liquid/gas interface initially presented in [7] are here briefly recalled. Introducing the harmonic perturbations, the ambient pressure is given by $p' = \hat{p}_C \exp(\mathrm{i}\omega t)$ and the mass flow rate by $\dot{M}' = \hat{\dot{M}} \exp(\mathrm{i}\omega t)$. Consequently, the equations of the gas phase (see subsection 2.3) imply:

$$\hat{\dot{M}} = \alpha \frac{\mathrm{i}u}{1+\mathrm{i}u}(\bar{b}\hat{T}_S - \hat{p}_C) \tag{17}$$

and:

$$\Delta\hat{Q}_L = \overline{\dot{M}}\,\bar{\ell}\,(\bar{a}\hat{p}_C - \mu\hat{T}_S) \tag{18}$$

where $u = 3\omega\bar{\tau}_v$ and $\Delta Q_L = \Delta\hat{Q}_L \exp(\mathrm{i}\omega t)$. The coefficients involved in these equations are:

$$\bar{a} = \frac{\bar{T}_C}{\bar{T}_C - \bar{T}_S}\frac{\gamma-1}{\gamma} + \varphi, \quad \bar{b} = \frac{\bar{T}_S}{(\bar{T}_S - c)^2}\,b, \qquad \mu = \frac{\bar{T}_S}{\bar{T}_C - \bar{T}_S} - \frac{2c}{\bar{T}_S - c} + \bar{b}\varphi$$

and $\alpha = \dfrac{\bar{B}_M}{(1+\bar{B}_M)\ln(1+\bar{B}_M)}\,\varphi$ with $\varphi = \dfrac{\bar{Y}_{AC}\bar{Y}_{FS}}{\bar{Y}_{AS}(\bar{Y}_{FS} - \bar{Y}_{FC})}\dfrac{\mathrm{M}_F}{\mathrm{M}_F \bar{X}_{FS} + \mathrm{M}_A \bar{X}_{AS}}$

The parameter γ stands for the constant isentropic coefficient and the latent heat of vaporization ℓ per unit mass of the liquid is given by: $\ell = b\,R\,T_S^2 / \mathrm{M}_F (T_S - c)^2$, where R denotes the universal gas constant.

3.3. *Mass response factor*

According to the Rayleigh criterion, when the ambient pressure perturbation $p' = (p - \bar{p})/\bar{p}$ induces a perturbation in the evaporating mass $q' = (q - \bar{q})/\bar{q}$, the mass response factor N is defined as $N = (|\hat{q}|/|\hat{p}|)\cos\phi$, where $|\hat{q}|$ and $|\hat{p}|$ are the moduli of mass release q and pressure p and ϕ is the phase difference between q' and p'. Therefore, a reduced mass response factor can be defined as the real part of the transfer function $Z = \hat{\dot{M}}/(\alpha\hat{p}_C)$. By using Equations (15)-(18) Z is deduced in function of u, θ and h as:

$$Z(u,\theta,h) = \frac{\mathrm{i}u}{1+\mathrm{i}u}\frac{A+\theta E(u,\theta,h)}{B-\theta E(u,\theta,h)} \tag{19}$$

where $A = 3(\overline{a}\overline{b} - \mu)/\lambda$ and $B = 3\mu/\lambda$ are some coefficients depending on $\lambda = c_L \overline{T}_S / \overline{\ell}$ and are related to the fuel physical properties. From now on, we will call 'response factor' the reduced response factor defined as the real part of the transfer function Z :

$$\frac{N}{\alpha} = \Re(Z) \tag{20}$$

4. Results and discussion

In this section, all the calculations and curves are performed with the fuel thermodynamic coefficients $A = 10$ and $B = 100$, corresponding approximately to orders of magnitude of values encountered in the classical fuels [7]. Thus, relatively to the heat transfer coefficient h that controls the feeding regime, and to the process characteristic times as defined in subsection 2.2, and again to the influence of the thermodynamic coefficients A and B, the mean droplet mass response factor will be analysed. Figure 2 shows response factor curves as functions of the reduced frequency $u = 3\omega\overline{\tau}_v$ for arbitrary values of the exchange ratio $\theta = \overline{\tau}_v / \tilde{\tau}_T$. The five columns of diagrams correspond respectively to five values of the heat transfer coefficient: $h = 0$; 0.1; 1; 10 and $+\infty$.

First, for $h = 0$ (Figures 2(a1), 2(a2) and 2(a3)) and for $h \to +\infty$ (Figures 2(e1), 2(e2) and 2(e3)), the response factor curves seem respectively like those of the adiabatic and of the isothermal injection regimes discussed in [3]. In fact, these curves are identical since, for a given value of the exchange ratio θ, calculations show that

$$E(u,\theta,h) \to \frac{\overline{s}_0\overline{r}_S \theta \sin(\overline{s}_0\overline{r}_S) + 2\theta\cos(\overline{s}_0\overline{r}_S) - 3\cos(\overline{s}_0\overline{r}_S) - 2\theta + 3}{\theta(1 - \cos(\overline{s}_0\overline{r}_S))} = E(u,\theta,0) \tag{21}$$

when $h \to 0$, while

$$E(u,\theta,h) \to -\frac{1}{2}\frac{2\theta s_0\overline{r}_S \sin(s_0\overline{r}_S) + 5\theta\cos(s_0\overline{r}_S) - 3\cos(s_0\overline{r}_S) - 5\theta + 3}{\theta(1 - \cos(s_0\overline{r}_S))} = E(u,\theta,+\infty) \tag{22}$$

as $h \to +\infty$. The function $E(u,\theta,h)$ is defined by Equation (16) and mentioned in Equation (19). The above expressions of $E(u,\theta,0)$ and $E(u,\theta,+\infty)$ correspond exactly to those used in the calculation of the complex transfer function Z as found for respectively adiabatic and isothermal feeding regimes in [3]. Hence, all the comparative results concerning the two extreme cases of injection highlighted in this latter reference are still valid for the present analysis.
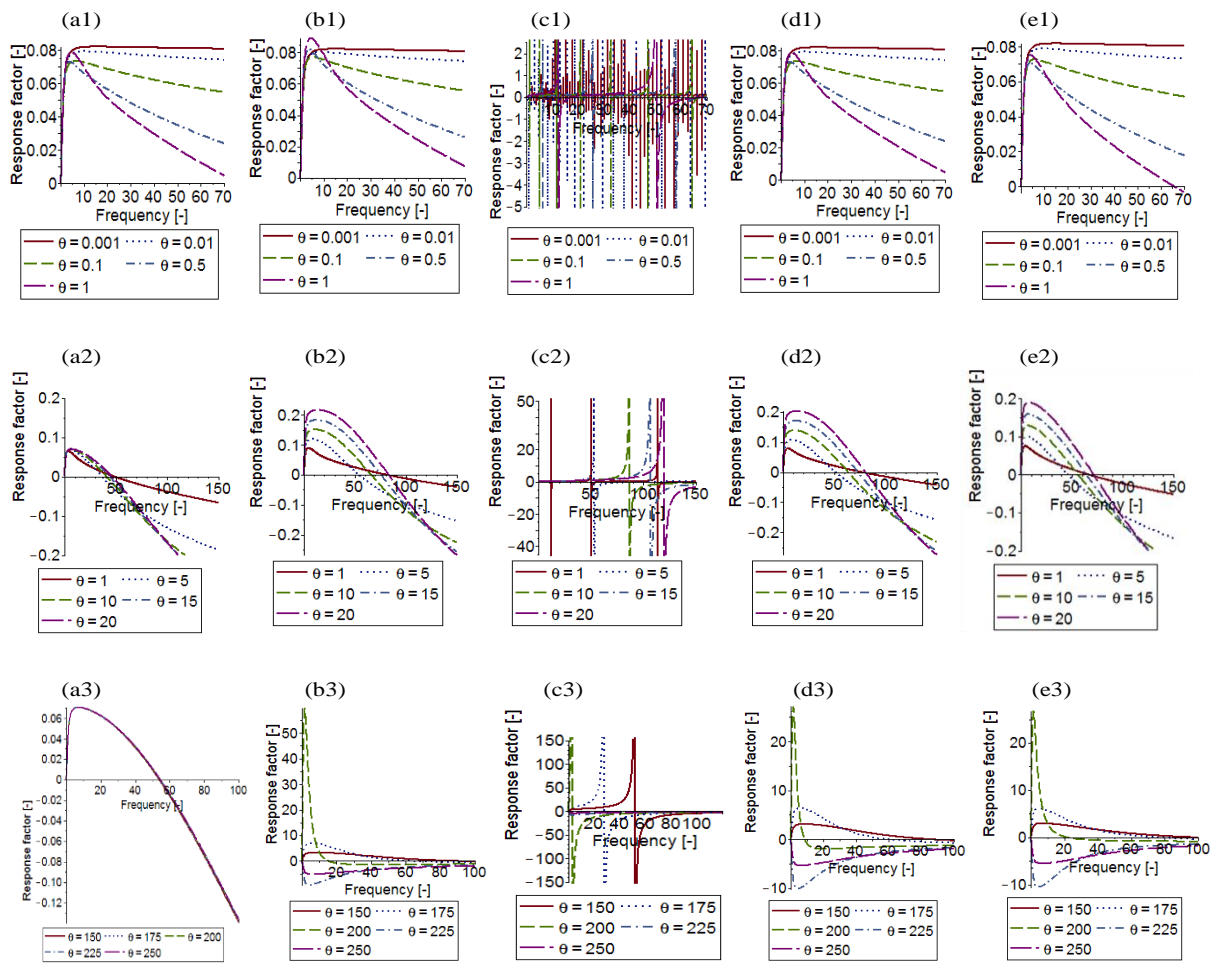
Figure 2. *Influence of heat transfer coefficient h on the reduced response factor N/α for different values of the exchange ratio θ for the mean spherical droplet model with $A=10$ and $B=100$. (a1), (a2) and (a3) for $h=0$ or adiabatic centre. (b1), (b2) and (b3) for $h=0.1$. (c1), (c2) and (c3) for $h=1$. (d1), (d2) and (d3) for $h=10$. (e1), (e2) and (e3) for $h=+\infty$ or isothermal centre.*

Secondly, according to Figures 2(c1), 2(c2) and 2(c3), the response factor curves show intriguing fluctuations in their profiles when the heat transfer coefficient h is fixed at one. In that case, when the exchange ratio θ is chosen lesser than one, the oscillations become straight chaotic although they appear relatively reduced in amplitude compared with the cases where θ is much greater than one. Indeed, keeping $h=1$ and increasing the value of the exchange ratio θ beyond one until a certain threshold value to be hereafter specified, a response factor line exhibits some hyperbolic pattern with high peaks value along the reduced frequency axis as in Figures 2(c2) and 2(c3). Moreover, once the heat transfer coefficient slightly differs from one, the curves tend to show more lower fluctuations in their profiles even if h remains very close to one as for $h=0.95$ or $h=1.05$, and many other examples not illustrated with figures. For comparison, a unity value of a heat transfer coefficient may characterise a radiation heat transfer processing from the flame to the chamber wall. According to [8] for example, the radiative power is highly nonlinear and varies at the first order as the fourth power of the local instantaneous temperature. It may be admitted that, even in fuel injection processes, this specific value of the liquid-liquid heat transfer coefficient ($h=1$) can strongly influence on the evaporating mass release response in a perturbed environment. At this point, experimental investigations are necessary for further clarifications.

Thirdly, for a given value of the exchange ratio θ, almost identical curve profiles are obtained when the not null transfer coefficient h remains much lesser than one as for $0 < h \leq 0.1$. Likewise, when $h \geq 10$, the response curve profiles seem unaffected by the variation of the transfer coefficient h at θ fixed. Indeed, Figures 2(d1), 2(d2) and 2(d3) for $h=10$ show very similar profiles

respectively with Figures 2(e1), 2(e2) and 2(e3) for $h=+\infty$. This behaviour can be explained by considering the expression of $E(u,\theta,h)$ defined by Equation (16) and the rate of variation of the term $\exp(\mathrm{i}\arctan h)=(\mathrm{i}h+1)/(h^2+1)^{1/2}$, precisely that of the inner function $\arctan h$ for $h>0$. Since its rate of variation near $h=0$ can be equated to one, the function $\arctan h$ tends rapidly enough to zero as h tends to zero. Consequently, the term $\exp(\mathrm{i}\arctan h)$ tends fast to one as h tends to zero. But, when h increases over one, the same function $\arctan h$ becomes asymptotically close to the value $\pi/2$ which is approximately reached as h approaches the value 10. Then, the term $\exp(\mathrm{i}\arctan h)$ tends slowly to the imaginary value i. On one hand, the first limit leads to the expression of $E(u,\theta,0)$, giving by Equation (21) and corresponding to the transfer function Z found in the adiabatic feeding case. As this convergence is rapid, the curve profiles, although unaffected by the variation of h in a deleted neighbourhood of zero, seem noticeably different from those obtained for the adiabatic injection regime ($h=0$). This is readily confirmed by comparisons of Figures 2(a2) and 2(a3) for $h=0$ with Figures 2(b2) and 2(b3) for $h=0.1$. On the other hand, the second limit leads to the expression of the function $E(u,\theta,+\infty)$ which intervenes in the isothermal injection transfer function (see Equation (22)). As the convergence is now asymptotic, the mass response factor curves for $h=10$ seem very similar to those obtained for the isothermal injection regime ($h=+\infty$). In brief, one may admit that whenever a not null heat transfer coefficient h is introduced in the injection process, high and nonlinear instabilities may intervene in the vaporization response. As a comparative example, the continuous supply of fuel to the chamber has been theoretically and experimentally identified as an important factor for producing or driving combustion instabilities [9, 10]. Finally, the rapid changes in the curve profiles leading to non positive response factor representations, especially for $h\geq10$, are not related to some particular values of the heat transfer coefficient but may rather be related to a specific value of the thermal exchange ratio θ as highlighted in [3]. A more detail analysis needs to be carried out also on this point.

5. Conclusion

Through the introduction of a heat transfer coefficient in the liquid fuel injection process, this study has extended to a more generalized feeding regime the results on the vaporization frequency response to ambient pressure oscillations. An idealized configuration of a mean droplet has permitted to compute the mass frequency response for a vaporizing spray. The effects of the liquid heat transfer coefficient are found effective for driven or dampen instabilities. Except for the case where the heat transfer coefficient is equal to one, the curves exhibit a single abrupt peak response whenever positive response exists in the system. The results are also found similar to those previously obtained in the adiabatic and isothermal feeding regimes. However, as shown by the present study, a chaotic vaporization frequency response may occur during subcritical combustion processes provided that certain specific boundary conditions are imposed. The results are also found similar to those previously obtained in the adiabatic and isothermal feeding regimes. Indeed, mass response factors in such extreme cases of fuel injection are recovered as simple limit points. The results obtained in this study can be easily generalized to many combustion systems, since the involved parameters are reduced and used in their non dimensional form. The above-mentioned results may be beneficial for instability control in combustion processes.

References

[1] V. Nair and R. I. Sujith, *Multifractality in combustion noise: Predicting an impending instability*, J. Fluid Mech. 747 (2014), pp. 635–655.

[2] S. Candel, D. Durox, T. Schuller, N. Darabiha, L. Hakim, and T. Schmitt, *Advances in combustion and propulsion applications*, Eur. J. Mech. B Fluids 40 (2013), pp. 87-106.

[3] K. Anani, R. Prud'homme, and M. N. Hounkonnou, *Dynamic response of a vaporizing spray to pressure oscillations: Approximate analytical solutions*, Combust. Flame 193 (2018), pp. 295-305.

[4] S.Y. Slavyanov and W. Lay, *The Heun class of equations*, in, *Special Functions: A Unified Theory Based on Singularities*, Oxford Mathematical Monographs Series, Oxford University Press Publishers, New York, 2000, pp. 97-162.

[5] M.F. Heidmann and P.R. Wieber, *Analysis of frequency response characteristics of propellant vaporization*, Tech. Rep. TN D-3749, NASA, Washington D.C., USA, 1966.

[6] B. Abramzon and W. A. Sirignano, *Droplet vaporization model for spray combustion calculations*, Int. J. Heat Mass Transfer 32(9) (1989), pp. 1605-1618.

[7] R. Prud'homme, M. Habiballah, L. Matuszewski, Y. Mauriot, and A. Nicole, *Theoretical analysis of dynamic response of a vaporizing droplet to a acoustic oscillation*, J. Propul. Power 26(1) (2010), pp. 74-83.

[8] R. G. D. Santos, M. Lecanu, S. Ducruix, O. Gicquel, E. Iacona, and D. Veynante, *Coupled large eddy simulations of turbulent combustion and radiative heat transfer*, Combust. Flame 152(3) (2008), pp. 387–400.

[9] Y. Xu, M. Zhai, P. Dong, F. Wang, and Q. Zhu, *Modeling of a self-excited pulse combustor and stability analysis*, Combust. Theory Modelling 15(5) (2011), pp. 623-643.

[10] A. Kannan, B. Chellappan, and S. Chakravarthy, *Flame-acoustic coupling of combustion instability in a non-premixed backward-facing step combustor: The role of acoustic-Reynolds stress*, Combust. Theory Modelling 20(4) (2016), pp. 658-682.